Fermi National Accelerator Laboratory

FERMILAB-TM-1909

Introduction to Colliding Beams at Fermilab

Joey Thompson

Fermi National Accelerator Laboratory
P.O. Box 500, Batavia, Illinois 60510

Department of Physics, University of Maryland
College Park, Maryland 20742

October 1994

Operated by Universities Research Association Inc. under Contract No. DE-AC02-76CHO3000 with the United States Department of Energy

Disclaimer

Introduction to Colliding Beams at Fermilab

Joey Thompson

Department of Physics, University of Maryland
College Park, MD 20742

The Fermi National Accelerator Laboratory is currently the site of the world's highest center-of-mass energy proton-antiproton colliding beam accelerator, the Tevatron. The CDF and DØ detectors each envelop one of two luminous regions in the collider, and are thus wholly dependent on the accelerator for their success. The Tevatron's high operating energy, reliability, and record setting integrated luminosity have allowed both experiments to make world-class measurements and defined the region of physics that each can explore. The following sections are an overview of the highlights of the accelerator operation and are compiled from many sources. The major sources for each section are listed at the beginning of that section.

1 Accelerator Overview

The Tevatron collider is the final stage in a series of seven accelerators that are necessary for colliding beams at Fermilab.[1][2] A Cockcroft-Walton preaccelerator, a linear accelerator (Linac), and a synchrotron (Booster) operate in series to produce 8 GeV protons for injection into the Main Ring synchrotron. The Main Ring has two purposes: it serves as the final boosting stage for protons and antiprotons before injection into the Tevatron, and it is the source of energetic protons which are used to create antiprotons when colliding beams are required. In addition, the Antiproton Debuncher and the Antiproton Source are used in collecting and cooling antiprotons for colliding beams. The overall layout of the accelerator complex is shown in Figure 1.

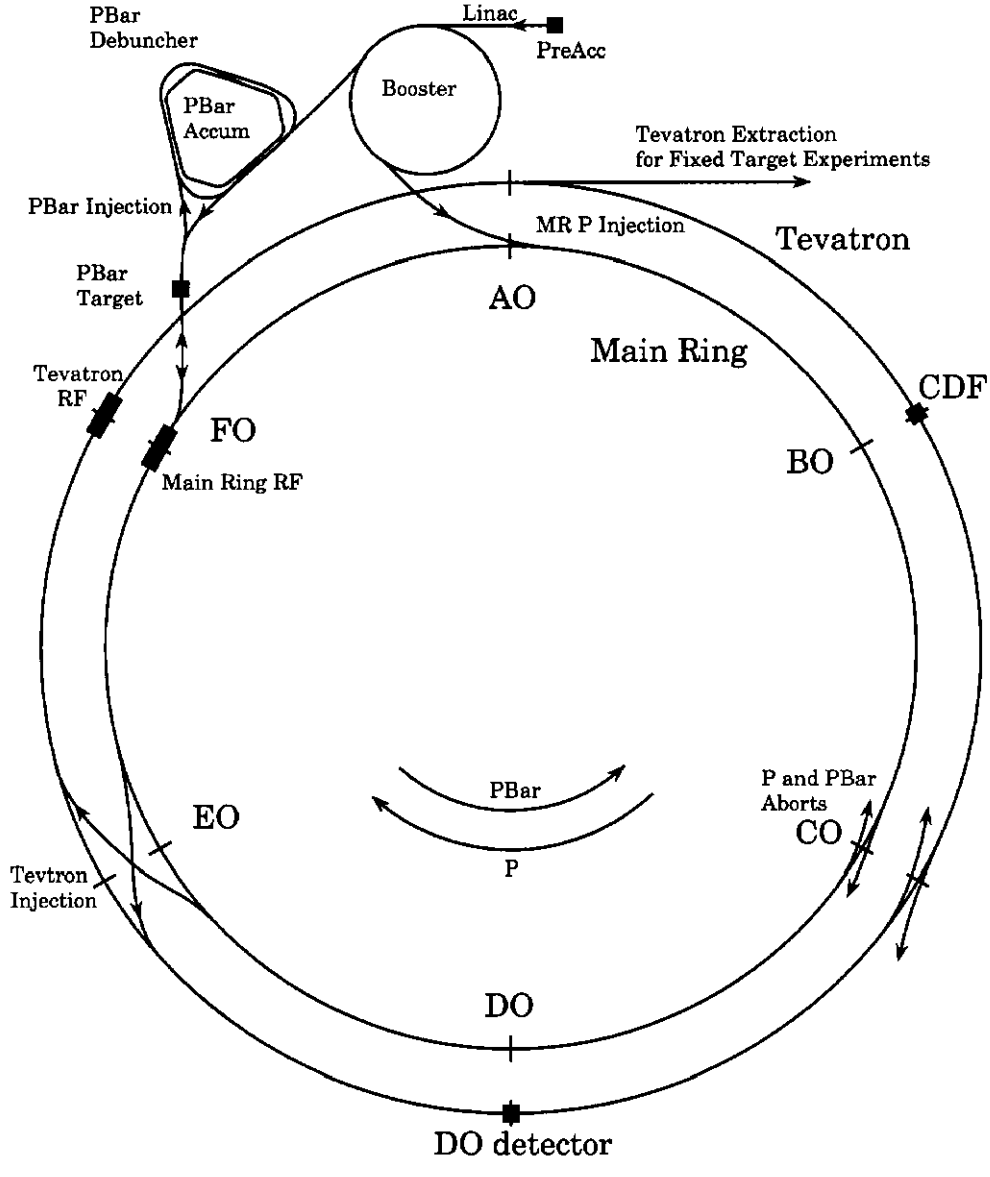

Figure 1 The general layout of the collider facility at Fermilab (not to scale). Note that the Main Ring and Tevatron are actually at the same radius but are shown separated in this figure for clarity.

Colliding beams in the Tevatron were first obtained in accelerator tests in October 1985 with a subsequent first operating run (for the CDF experiment) in early 1987. DØ recorded its first collider data during the third operating run of the Tevatron.

2 The Preaccelerator

The preaccelerators (there are two for redundancy) each consist of a negative hydrogen ion source, a Cockcroft-Walton generator, an electrostatic accelerating column, and a transport line which injects the beam into the Linac.[3] Negative hydrogen ions are produced at 18 keV in the source and accelerated through a 750 kV potential as they pass from the ion source through a seven gap DC accelerating column to the preaccelerator enclosure wall and transport line which are at ground potential. The ion source and all associated systems necessary to operate the source are located within a metal enclosure ("dome") kept at -750 kV by a commercial five stage dual-leg Cockcroft-Walton generator. After being accelerated to 750 keV, the beam passes through an electrostatic chopper in the transport line which controls the amount of beam current that passes to the Linac by sweeping away the unwanted portion of the pulsed beam coming from the source. As well as steering and focussing magnets and various beam diagnostic devices, the transport line also includes a single gap RF cavity which bunches the beam at 201.24 MHz (the RF frequency of the Linac) to raise the capture efficiency in the Linac to about 70% (from ~35% for nonbunched beam). Further descriptions of the ion source and the Cockcroft-Walton generator are provided below.

2.1 Negative Hydrogen Ion Source

The proton beam in the Main Ring begins life as a pulsed 18 keV 50 mA negative hydrogen ion beam from a magnetron surface-plasma source.[4] This type of source became operational at Fermilab in March, 1978 when it replaced a higher current H^+ duoplasmatron; a replacement was necessary to increase the beam quality in the Booster.

A basic magnetron source is shown in Figure 2[5]. It consists of an oval-shaped cathode surrounded by an anode with a magnetic field passing through the apparatus. Hydrogen gas is added to a pressure of a few hundred millitorr. The combination of nonvarying magnetic and electric fields produces a dense plasma while confining the electrons to spiral within the anode-cathode gap (typically about 1 mm). The cathode is the active surface for producing H^- ions. Positive ions and energetic particles strike the cathode and sputter off hydrogen atoms which have been absorbed on the

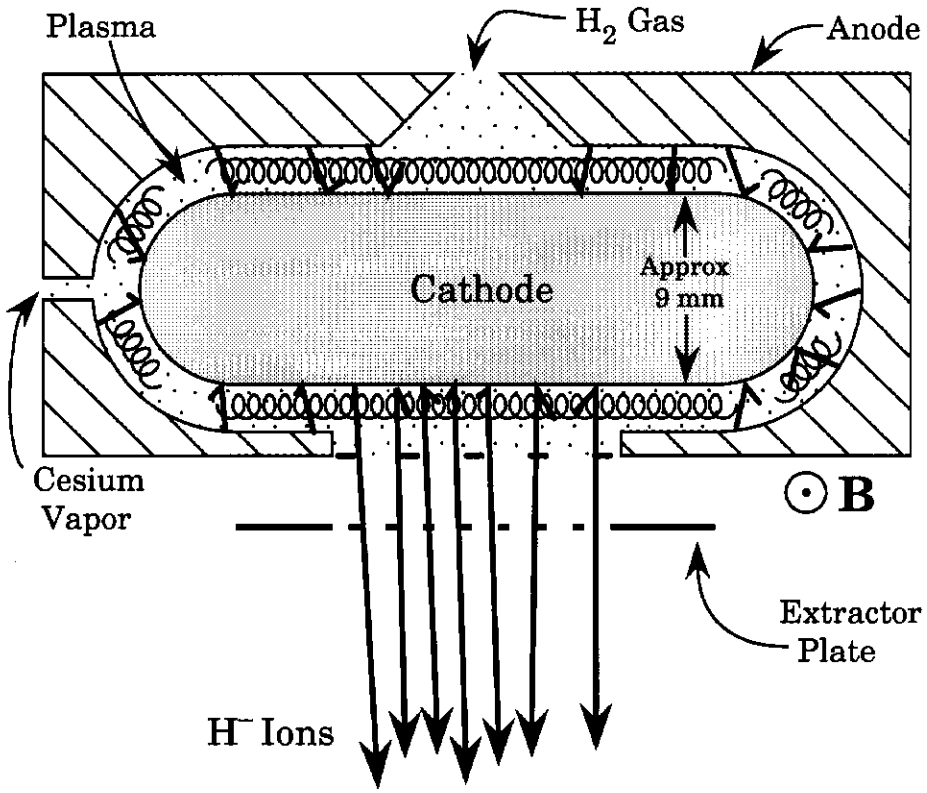

Figure 2 The basic configuration of a magnetron source[5]

surface. A smaller contribution to the H^- production comes from positive hydrogen ions which reflect from the cathode after acquiring two electrons.[6] Hydrogen atoms leaving the surface of the cathode normally have a small chance (<0.2%) of removing the necessary electrons; the addition of Cesium vapor to coat the cathode surface (about 0.6 monolayers thick) lowers the work function of the surface and raises the efficiency of the process to nearly 10%. Cesium also has the benefit of ionizing easily thereby improving the source stability. After formation, some of the H^- ions are extracted through the anode aperture and are accelerated through the extraction plate. Electrons and other ions which escape are eliminated by magnetically steering the beam through a right-angle bend.

The Fermilab source operates in a pulsed mode where the hydrogen gas input, the plasma discharge voltage, and the extraction voltage are pulsed at a rate of 15 Hz which matches the Linac cycle and results in longer source lifetime. Typical operation yields a pulse duration of approximately 80 μsec. The electrical isolation

required to operate the source at high potential requires that the source control system communicate with the outside world via an optical link. Electrical power for the system is provided by a 15 kW alternator located within the dome and driven by an electrically isolating G-10 shaft which is externally driven.

2.2 The Cockcroft-Walton Generator[3]

The high voltage for the electrostatic accelerating column is produced by a commercial Cockcroft-Walton generator which is arguably the most interesting-looking device at Fermilab. This is a solid state device which generates high voltage by charging capacitors in parallel from an AC voltage source and discharging them in series, a feat made possible by the judicious placement of diodes. A simple diode voltage multiplier is shown in Figure 3. This type of circuit is also the core of many high voltage supplies used in high energy experiments.

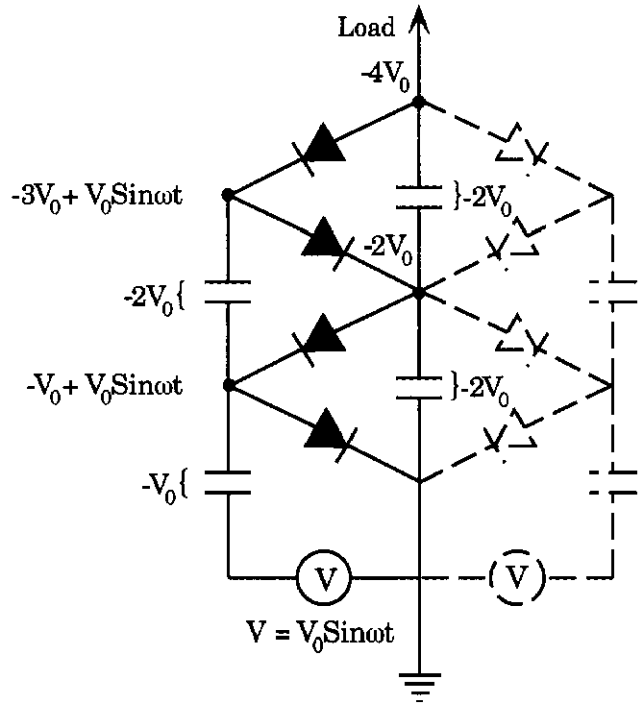

Figure 3 A schematic for a simple two-stage diode voltage multiplier (filled lines) is shown.[3] Note that each stage of the chain adds $2V_0$ to the output voltage. The dotted lines represent the addition of a second leg as is done for the Fermilab dual-leg five-stage Cockcroft-Walton. This yields the same output voltage with less ripple.

The preaccelerator Cockcroft-Walton has five stages which result in a factor of ten increase in the maximum input voltage provided by two transformers with 75 kV on the secondaries. In contrast to a standard Cockcroft-Walton, a second leg on the diode multiplier ladder is added to the Fermilab high voltage source in an effort to halve the output voltage ripple.

3 The Linac

The Linac is a two-stage linear accelerator that produces a pulsed beam of 400 MeV H^- ions for charge-exchange injection into the Booster.[3][7][8][9] The first stage of the Linac, an Alvarez drift-tube accelerator, accelerates the ions to 116 MeV. A new (1993) side-coupled linac replaced a portion (67 m) of the original 200 MeV drift tube linac and currently operates in tandem to accelerate the beam to the full energy of 400 MeV.

The Alvarez drift-tube linac is about 79 m long and accelerates the ions in five (formerly nine) electrically resonant cylindrical OFHC (Oxygen Free High Conductivity) copper clad steel tanks. Each RF tank resonates at 201.24 MHz and is driven by its own RF system producing 5 MW of power in 400 μsec pulses phase locked to the Booster cycle of 15 Hz. The interior of each tank consists of a line of n full drift tubes (where $23 \leq n \leq 59$) suspended in the radial center of the tank with bore holes through which the beam passes as shown in Figure 4. (There is an additional half drift tube at either end of each tank.) The cavity design is such that there are $n+1$ resonant cells within the tank with each cell extending longitudinally between two imaginary walls at the center of two adjacent drift tubes. Each drift tube is separated from the next by a gap. Particles within this gap region are affected by the field in the tank; within the drift tube, the bunches are shielded from the RF.

For effective acceleration, a particle which travels down the Linac should always experience an accelerating field while in the gap between drift tubes; the subsequent decelerating field should occur while the particle is shielded within a drift tube. One defines the phase of the particle as the phase of the electric field when the particle passes through the center of the resonant cell. The synchronous phase angle ϕ_s is then defined as the one phase for which the particle will reach the center of the next cell just as the RF has passed through 360°. Maximum accelerating efficiency then

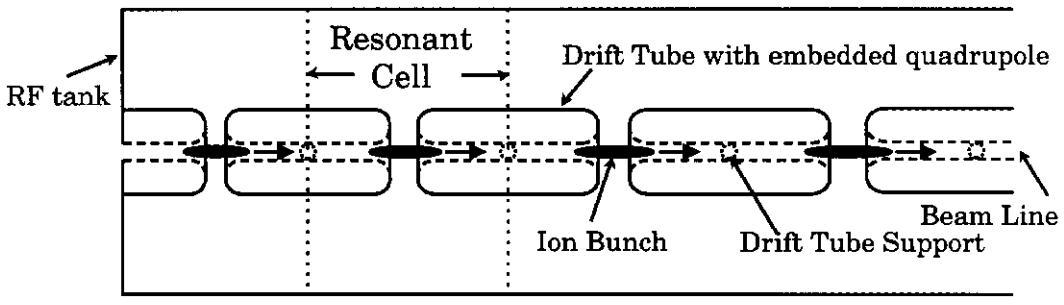

Figure 4 A top view of a simple Alvarez drift tube linac. Note that each RF bucket is filled with a particle bunch.[3]

occurs when the accelerating field is at a maximum while the particle is in the gap (i.e. when $\phi_s = 0$). However, for nonrelativistic particles, this choice for ϕ_s would result in very low transport efficiency through the Linac. Particles arriving late (slower particles) would experience a smaller increase in energy than the synchronous particles and would thus be even slower to arrive in the next cell; these are eventually lost. Particles arriving early (faster particles) would be appropriately slowed, but they are also in peril of being lost if their resultant phase angle should fall below zero. A compromise between accelerating efficiency and transport efficiency is made with $\phi_s = -32°$. Thus, particles arriving late (slower) receive more energy than the synchronous particle, and particles arriving early (faster) receive less. This creates a stable phase region in the Linac of about 105°. (This is ≈35% of the total phase and is the source of the capture efficiency for nonbunched beam in the Linac quoted earlier.) Another effect due to the nonrelativistic nature of the beam is that since the speed of the ions increases as they progress down the Linac, the resonant cells become progressively longer so that the beam can maintain a constant phase with respect to the accelerating field within the cells. Finally, an additional complication arises due to space charge and RF effects which tend to blow up the beam. This is countered with the presence of alternating focussing and defocussing quadrupole magnets embedded within the drift tubes themselves.

The new side-coupled section of the linac operates on the beam in the same fashion as the drift-tube linac. Its cavities are designed differently to be more efficient and resonate with the fourth multiple of the drift-tube linac, ≈805 MHz. Thus in this section, every fourth RF cycle (bucket) contains beam particles. RF power is obtained from seven 10 MW, 805 MHz klystrons. Transverse focussing is achieved by quadrupoles between each cavity in a FODO lattice (focussing, drift, defocussing, drift...).[6]

4 The Booster

The Booster is an 8 GeV fast cycling proton synchrotron which serves as an injector for the Main Ring.[10][11][12] It accelerates 400 MeV protons obtained from the Linac via multiturn charge-exchange injection at a rate of 15 Hz.[13] A set of 96 combined function dipole/quadrupole magnets along with 17 dual gap ferrite-tuned cavity resonators arranged around its 151 m diameter form the basic structure of the Booster.

Prior to the Fermilab Main Ring, many proton synchrotrons used a linac as an injector. This was impractical for the Main Ring because linacs at the time were unable to produce a proton beam energy above a few hundred MeV given reasonable size constraints. This energy regime presented a problem of dynamic range for the Main Ring which was to produce protons at 400 GeV. The chosen solution was a small booster synchrotron accelerator which would fill the Main Ring in several cycles. A synchrotron is an accelerator where the particles follow a closed orbit while being accelerated via multiple passes through accelerating stations; this requires that the magnetic fields constraining the particles to their orbits and the RF fields accelerating the particles vary synchronously with the change in particle momentum.

The typical momentum spread of the Linac H^- beam ($\sim$0.3%) corresponds to an orbit radius difference of $\sim$8 mm in the Booster; it contributes to filling the limited aperture of the Booster and complicates beam capture.[14] An RF debuncher is thus placed at the end of the Linac transport line to minimize the momentum spread of the beam. (There is no penalty associated with debunching the beam since the RF structure of the beam emerging from the Linac is incompatible with that of the Booster.) The debuncher is simply an RF cavity phased with respect to the incoming bunches such that it decelerates fast particles and accelerates slower particles. This is possible because the bunches separate according to their momentum as they coast down the 46 m transport line.

During injection, the RF accelerating fields present in the Booster's RF cavities are phased with respect to one another so that there is no net acceleration of the beam. Injection could then proceed by firing protons into the Booster for a single "turn" (the time required for one complete revolution of a particle in orbit in the accelerator) while the protons coast in the ring. In fact, better performance has been obtained with multiturn charge-exchange injection as depicted in Figure 5. In this system,

negative hydrogen ions are brought into a parallel path with a closed orbit for protons in a straight section of the booster. The two beams are merged by passing both through a dogleg (two adjacent dipole magnets of opposite polarity). The merged beam then passes through a carbon foil which strips electrons from the negative hydrogen ions. Another dogleg (or Orbital Bump magnet) restores the original proton beam with the newcomers to the proper closed orbit of the machine while allowing unstripped ions to pass to the beam dump. The charge-exchange represents a non-conservative action and thus allows the two beams to be absolutely merged, an act that would otherwise violate Liouville's Theorem. The Booster is typically filled in six turns (about 3×10^{12} protons)[15] after which the Orbital Bump magnets are powered off to reduce beam loss due to scatter in the foil. The amount of time spent filling the Booster is selected via an electrostatic chopper at the end of the Linac.

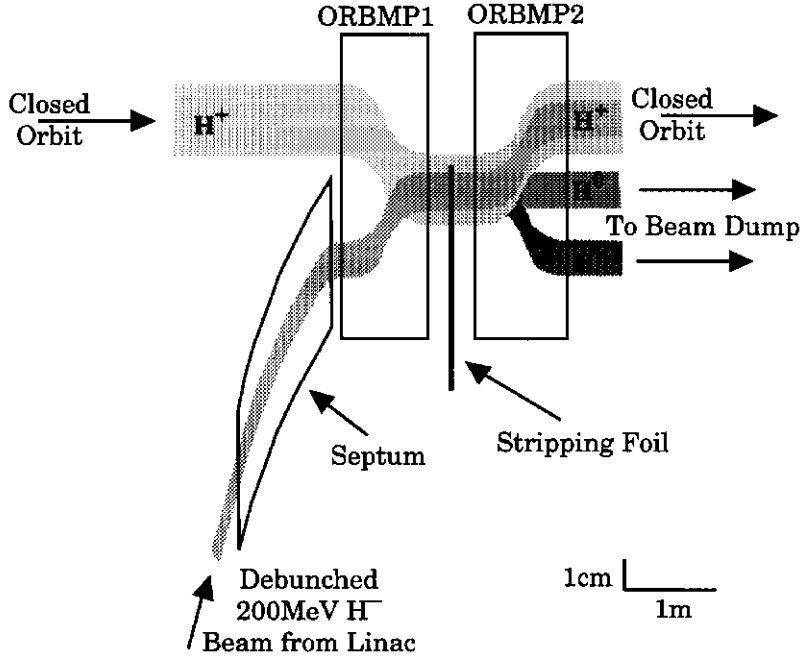

Figure 5 A simplified view of the Fermilab Booster injection area for H^- multiturn charge-exchange injection.

Once the Booster is filled, the RF stations are brought into proper phase over a period of 100-200 μsec. This captures the beam into the RF bucket structure of the Booster. The beam is then accelerated to its final energy of 8 GeV by varying the RF frequency from 37.9 MHz at injection to 52.813 MHz (phase locked to the Main Ring RF) at extraction; the RF variation is synchronous with the ramping of the magnet

currents. The resonant frequency of the cavities is adjusted concurrently with the frequency of the sine-wave output of the 100 kW power amplifiers driving them by varying the bias supply current (and thereby the inductance) of ferrite tuners linked to the cavities. The entire acceleration takes ~33 msec, and the Booster cycles in ~66 msec (15 Hz).

The frequency with which the Booster completes the acceleration cycle requires that the magnets be an integral part of a resonant system. Each of the bending magnets in the Booster is a combined function dipole/quadrupole. Two such magnets (focussing and defocussing) are combined in one module with a capacitor bank and a choke completing an LC circuit which resonates at 15 Hz. A biased sine wave of 15 Hz is applied to the magnets with injection occurring during the time of lowest magnet current. (This is, not coincidentally, an integral fraction of the 60 Hz line frequency from the power company. The booster is phase-locked to the incoming power.)

Just as in the Linac, the bunches orbiting in the synchrotron must be properly phased with respect to the RF fields present in the accelerating gaps for effective operation. This requires that there be an integral number of RF buckets (or possible bunch locations) in a closed orbit. There are 84 RF buckets in the Booster; that is, the RF system has a *harmonic number* of 84. During extraction, "kicker" magnets are pulsed for ~1.6 μsec to extract the entire beam in one turn ("fast extraction"). The rise time of these magnets (~30 nsec) is such that one of the bunches is lost in the process.

The Booster operates in two modes for colliding beam operations. When the Booster is accelerating protons for eventual injection into the Tevatron, only 11, 13, or 15 bunches are actually injected into the Main Ring for final coalescing into one bunch. The rest of the buckets are directed to a beam dump. While antiprotons are being collected, the Booster delivers one full turn (or "batch") of protons (84 – 1 = 83 bunches) to the Main Ring approximately every 2.4 sec.

One interesting relativistic phenomenon called "transition" occurs in the Booster. As in the Linac RF system, proper phasing of the RF with respect to the bunch crossing ensures a stable region (longitudinally) for the bunch. As the acceleration cycle begins, after the beam is injected and captured, those particles that have lower energy than the synchronous particle (as described in 3 above) arrive late and experience a larger accelerating field than the synchronous particle. Higher energy parti-

cles arrive early and experience a smaller accelerating field. This creates a bunch that is longitudinally stable or stable about the synchronous phase angle. (Oscillations about this stable phase angle are known as synchrotron oscillations.) The situation is very different at higher energies. For very high energies, the particles with higher momentum do not travel significantly faster than the particles with less momentum in the bunch because they are all asymptotically approaching the speed of light. However, this added momentum still results in the higher energy particles following a larger radius orbit. Since they do not have significantly greater speed than their low momentum counterparts, this path difference causes the higher energy particles to have a longer transit time around the ring! If the phase of the RF was left the same as it was shortly after injection, the higher energy particles (which are now arriving *later* than the synchronous particle) would receive even more energy; the lower energy particles would receive less. What was formerly a restoring force within the bunch would become a destabilizing force, and beam would be lost. The point in an accelerator cycle at which this change in arrival times occurs is known simply as "transition." The phase of the RF accelerating fields must be changed appropriately as the accelerator passes through transition to maintain a stable bunch. Transition occurs when the protons have a kinetic energy of ≈4.2 GeV ($\gamma_t = 1/(\sqrt{1 - v^2/c^2}) \approx 5.45$) in the Booster. Clearly, this is a region of beam instability, and this part of the cycle must be passed through quickly. The Booster is unique in that it has a special set of quadrupoles with a fast rise time which change the transition energy of the accelerator as it approaches transition such that the transition energy is pushed quickly below the current beam energy.

One other topic that should be mentioned for completeness is betatron oscillations (taken from the betatron machines in which they were first observed) which are stable oscillations in the transverse direction about the ideal closed orbit of a circular accelerator. The stability is no accident. It is provided by an alternating series of quadrupole magnets. Because of the field gradients in a quadrupole, such magnets can be regarded as analogous to simple lenses in optics in that the focussing or defocussing effect is proportional to a particle's radial distance from the axial center of the magnet; the analogy is not complete however since a beam passing axially through a quadrupole is subject to a focussing force in one transverse dimension and a defocussing force in the other transverse dimension. Fortunately, if quadrupoles are alternated (focussing and defocussing as defined in one dimension, usually the

horizontal) with the proper spacing, a net focussing effect occurs. This is done for all of the circular accelerators at Fermilab with different types and placement of quadrupoles specifically designed for each machine. Because the beam focussing is accomplished with alternating quadrupoles, this type of machine is properly known as an alternating gradient synchrotron. The *tune* of such a machine is the number of betatron oscillations that the beam undergoes in one complete orbit of the machine; the tune is given separately for the vertical and horizontal directions. The *beta* function for a machine is related to the lattice of quadrupoles in the machine and is proportional to the instantaneous (since β is a function of position) wavelength of the betatron oscillations (in a perfect machine). Note that β is quoted for the vertical and horizontal directions separately since the focussing is different in the two dimensions. The beta function (x and y) is also a parameter governing the transverse size of the beam. Thus, in a region of low beta, the beam spot size in a machine is smaller than elsewhere.

Finally it is worth noting that the linac upgrade was motivated by a desire to increase beam current in the booster with the ultimate goal being increased luminosity in the Tevatron. As the total charge in a circular accelerator increases, space charge forces tend to defocus the beam. This is manifested in a downward tune shift (a lowering of the number of betatron oscillations occuring in one complete orbit) which is approximately proportional to the number of particles in the beam and the radius of the accelerator and inversely proportional to $(v/c)\gamma^2$. The last term indicates that the tune shift is largest at low energies; thus increasing the injection energy of the booster is a straightforward cure for beam losses due to space charge effects.

5 The Main Ring

The Main Ring is a 400 GeV proton synchrotron with a radius of 1000 m.[16] Prior to the commissioning of the Tevatron in July, 1983, the Main Ring was the highest energy accelerator in the world. Now it serves as a 150 GeV injector of protons and antiprotons for the Tevatron as well as a source of 120 GeV protons used in antiproton creation. It is composed primarily of 774 dipole magnets, 240 quadrupole magnets, and 18 dual gap RF cavities; it contains 1113 RF buckets and operates at about 53 MHz. The layout of the Main Ring can be seen in Figure 1 above, where the labels

denote straight sections used for the placement of injection and extraction lines, RF cavities, and colliding beam experiments. The Main Ring operating modes for colliding beams are described below.

The two major deviations from a circular orbit in the Main Ring are two excursions vertically out of the plane of the circle at B0 and D0. The design of the Tevatron (originally called the Energy Saver because of its superconducting magnets) was constrained by the requirement that it should be installed within the existing Main Ring tunnel. The Energy Saver magnets are located at the same radius and a little more than two feet below the magnets of the Main Ring. The exceptions to this are "overpasses" built for the Main Ring at the B0 and D0 interaction regions where the Main Ring beamline is separated vertically from the Energy Saver ring. The overpass was envisioned to allow collider experiments located in these two regions to operate without the irritation of an additional hole through their detector. It also has the advantage of allowing the Main Ring to operate continuously (making antiprotons) during a colliding beam store without disturbing the physics potential of one of these detectors. The CDF detector (located at B0) was the first large collider detector at Fermilab; thus, the overpass built at B0 was designed to bypass the large detector completely with a vertical separation of approximately 19 feet. Such a large separation required major changes to the Main Ring tunnel. The overpass at D0 served originally as a prototype for the B0 overpass with the understanding that another collider detector would eventually take advantage of the separation.[16] The decision was made to limit the vertical separation at D0 to what could be obtained without major tunnel modifications, 89.2 inches. This is the source of the infamous Main Ring hole in the DØ detector.

5.1 Tevatron Injection

First the Main Ring must "capture" the beam injected from the Booster or the pbar source. (Note that these circulate in opposite directions.) Even though the bunch structure of the incoming beam is phase locked to the RF structure of the Main Ring, all is not simple. The RF buckets must match in phase space (technically, they must match in shape the invariant phase space contours accepted by the Main Ring accelerator lattice[17]), not just in longitudinal position as is accomplished with the RF phase lock. One aspect of Booster injection into the Main Ring provides a concrete

example of this. Low momentum particles circulating in the Booster are in the inside of the ideal orbit. If no provision is made to match the transverse position/momentum of off-momentum particles in the bunch, these slower particles would end up on the outside of the Main Ring ideal orbit which would result in extremely lossy transfers. (See Figure 1.) While this problem is addressed in the Main Ring injection lines, the difficulty of the problem combined with poor magnetic field quality in the Main Ring at 8 GeV results in large losses at injection.

Once captured at 8 GeV, the beam is accelerated to the Tevatron injection energy of 150 GeV during which the resonant frequency of the RF cavities is varied from 52.8 MHz to 53.1 MHz via the use of ferrite tuners as were used in the Booster. During the process, the Main Ring beam passes through transition at 17.6 GeV; this marks another period of heavy losses. The timing of the injection cycle is shown in Figure 6 where "flattop" denotes the time during which the beam is at its maximum momentum and the magnet currents are held constant. Once at flattop, two tasks must be accomplished: coalescing and cogging.

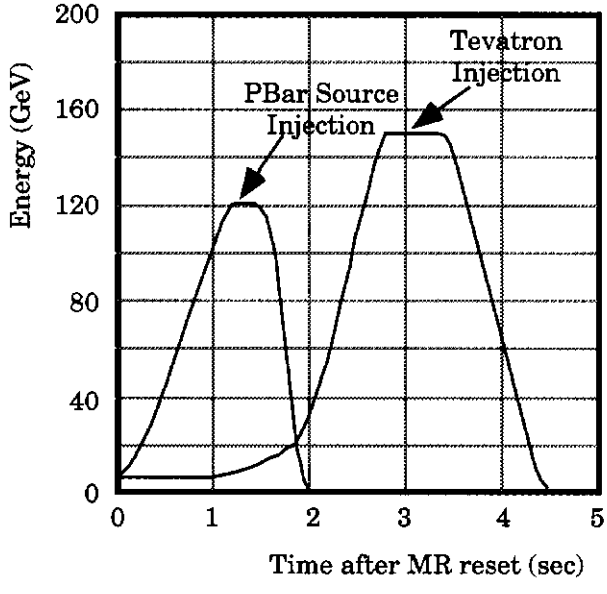

Figure 6 The Main Ring cycle for pbar stacking and Tev injection.

In its role as an injector for colliding beams in the Tevatron, the Main Ring must maximize the number of particles in a bunch transferred to the Tevatron and place each bunch in the appropriate Tevatron RF bucket. Because the number of particles in the Booster and pbar Accumulator bunches is too small for a collider bunch, the

Main Ring is forced to "coalesce" several bunches into one prior to injecting into the Tevatron. Once flattop is reached, the 53 MHz RF is counterphased (where adjacent RF stations are out of phase by 180°) to allow the bunches to cross RF bucket boundaries. Seven coalescing cavities are then turned on with some operating at 2.5 MHz and others operating at 5 MHz. They are phased such that the addition of the effect of the two waveforms will produce an effective resultant waveform which is linear through the region where the odd number of low intensity bunches to be coalesced reside. This is shown in Figure 7. Once the bunches are crossing at the central bunch, the 53 MHz RF is restored, recapturing the coalesced bunch while the coalescing cavities are turned off. Fifteen Booster bunches were injected into the Main Ring for coalescing for collider stores for Run 1A; only eleven buckets were injected from the pbar source to minimize antiproton loss since coalescing efficiency drops rapidly beyond this number of input buckets. Coalescing results in typical proton bunches of $\sim 150 \times 10^9$ particles with antiproton bunches having only $\sim 50 \times 10^9$ particles.

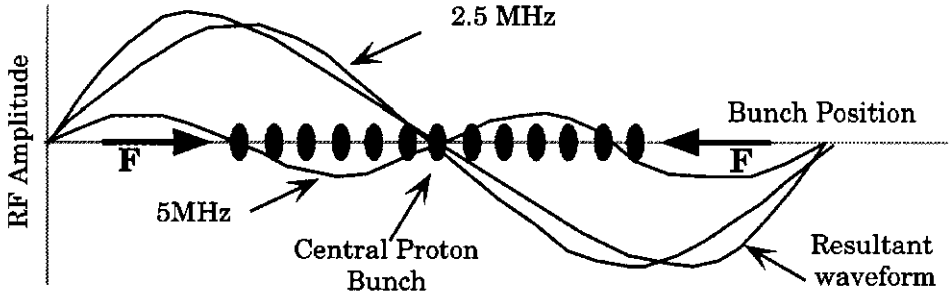

Figure 7 The effect of coalescing in the Main Ring. Note the linear restoring force induced by the combined RF fields of the coalescing cavities which causes all bunches to cross the central bunch at the same time.

Once coalescing results in one bunch, cogging is used to align the bunch in the Main Ring for injection into the assigned spot in the Tevatron. Prior to injection, the Main Ring and Tevatron RF systems are phase locked. Both the Main Ring and the Tevatron circulate timing signals known as Beam Sync (MRBS for Main Ring and TVBS for Tevatron.) The bunch positions in each machine are known relative to each machine's Beam Sync. The process of cogging then uses a digital phase shifter applied to the Main Ring RF system to "rotate" the phase of the beam in the Main

Ring relative to the beam in the Tevatron, thereby aligning the MRBS and TVBS markers (requiring a specific time difference between the two) for injecting the coalesced bunch into the appropriate Tevatron RF bucket.

5.1.1 Pbar Stacking

The Main Ring also operates as a source of 120 GeV protons which are extracted onto a Nickel target for antiproton production (known as pbar stacking); this is its major task during collider running. The Main Ring completes a pbar cycle in 2.4 sec as seen in Figure 6 and usually begins a new cycle immediately (though the period is not fixed and may be longer.) Note that after pausing to attend to its duties as an injector, the Main Ring continues producing antiprotons while the Tevatron contains a colliding beam store. This is to replenish the antiproton stack for the next Tevatron store.

Just as in the injector mode, the Main Ring must capture and accelerate protons from the Booster, experiencing losses primarily during injection and transition.[23] Transition occurs ~0.3 sec after the start of the cycle with flattop occurring about 1.2 sec later (see Figure 6). In the pbar stacking mode, the Main Ring accepts one full Booster batch (about 83 buckets or $83/1113 \sim 7.5\%$ of the Main Ring). Once flattop is reached, the bunches are rotated in phase space by the judicious use of counterphasing such that they each become narrow in time but large in momentum spread. (The RF voltage is reduced while adjacent cavities are counterphased. During the following 8 msec, the bunches stretch occupying a large time spread and a small momentum spread. The RF is then quickly returned to normal and the bunches begin their synchrotron oscillations. After approximately 1.2 msec, the bunches have rotated 90° in phase space reversing the time and momentum spread; thus the bunches have a smaller time spread and a larger momentum spread.)[18] At this point the beam is extracted onto the pbar target.

6 The Antiproton Source

The Antiproton Source was the last major component of the accelerator system to be constructed.[2][18][19] The Tevatron was operational at Fermilab as a source of protons for fixed target experiments prior to the construction of the Antiproton Source, but

colliding beam experiments with their much higher center-of-mass energy were required to satisfy the major physics goals of the late 1970s. The Tevatron was originally designed with this future expansion in mind. Colliding hadron beams can be accomplished in two obvious ways: proton-proton, or proton-antiproton. While a proton-proton collider (like the ill-fated SSC) offers the advantage of having hydrogen gas as the source of both beams, it has the major economic disadvantage of requiring two accelerators for the counter-rotating beams. A proton-antiproton collider can have both beams counter-rotating in the same beampipe because of their opposite charge. Thus the Antiproton Source was born as a source of antiprotons since none are readily available.

The Antiproton Source is comprised of a target station, a Debuncher ring and an Accumulator ring, and the transport lines associated with these devices. The components are briefly described below; however, the antiproton source is quite complicated and far beyond the scope of this overview. An excellent (!) review is available in the literature.[19] The accumulation of antiprotons involves extracting protons from the Main Ring, directing them onto a target, collecting negatively charged particles with an ≈8 GeV momentum from the secondaries, and "cooling" the antiprotons so that they may be stored for later use in the Tevatron. This process continues for several hours until sufficient antiprotons are available for later injection into the Tevatron. The Debuncher and Accumulator rings, with the placement of their stochastic cooling[20] systems, are shown in Figure 8.

6.1 The Antiproton Target

The Antiproton Target is used for creating the antiprotons. The process begins as described in 5.1.1, where about 83 bunches of 120 GeV protons with a small time spread are extracted from the Main Ring and directed onto a nickel target disk.[15] (Nickel is currently used, but other target materials are available and have been used.) The disk can be positioned such that the beam passes through the desired chord length for optimum antiproton production. Antiprotons of 8 GeV were used for simplicity since that was already the standard injection energy of Booster protons into the Main Ring. Antiprotons of this energy regime are most effectively produced by a proton beam near 120 GeV. About 10^7 antiprotons are produced for every 10^{12} protons striking the target.

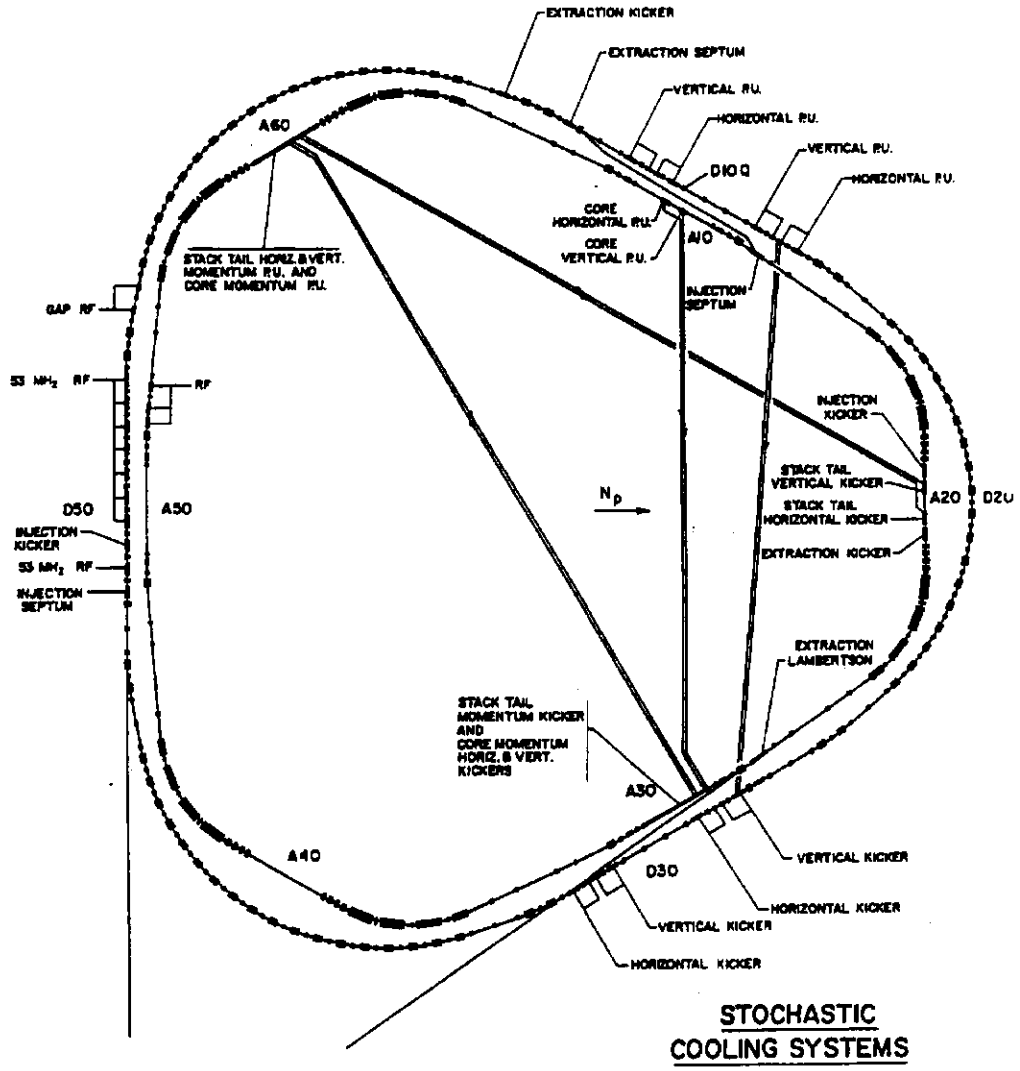

Figure 8 The Accumulator and Debuncher rings showing the placement of their stochastic cooling systems.[2]

The particulars of the proton targeting are important for minimizing the emittance of the collected antiprotons and thus the complexity and expense of the collection system. (*Emittance* in each dimension is the phase space area containing a certain fraction, often 95%, of the beam.) The angular distribution of the antiprotons emerging from the target is clearly determined by the kinematics of the production process. However, the spatial distribution of the antiprotons is given by the proton beam spot size at the target. Thus minimizing the proton beam spot size from the Main

Ring helps to minimize the phase space occupied by the antiprotons emerging from the target. At the target, the beam size has a radius $r \approx 0.15$ mm.

The narrow time spread of the proton beam impinging on the target also helps to maximize the phase space density of the resultant antiprotons which lessens the demands on the stochastic cooling system later. While the maximum antiproton production efficiency occurs for antiprotons produced at rest in the center of mass system of the proton-nucleon system (7.5 GeV for 120 GeV proton beam), the variation in production cross section is small about this maximum. Thus, there is no significant benefit to minimizing the momentum spread of the incoming proton beam since the momentum spread of the emerging antiprotons will not be substantially altered. Rather, the longitudinal emittance of the beam is minimized by minimizing the time spread of the impinging proton bunch as described in 5.1.1.

A cylindrical lithium lens (15 cm long x 1 cm radius) is placed immediately after the target and acts to focus the secondary particles along paths parallel to the axis of the cylinder as shown in Figure 9. A pulsed current of ~0.5 MA (!) is passed longitudinally through the lithium creating an azimuthal magnetic field which accounts for its focussing effect. Lithium was chosen because it is the least-dense solid conductor which reduces the occurrence of antiproton absorption and multiple scattering.[2]

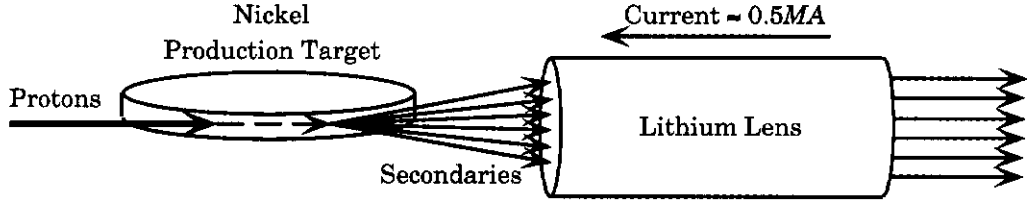

Figure 9 A simple drawing depicting the operation of the lithium lens in the target station.[18]

Following the lens is a pulsed dipole magnet which selects 8 GeV negatively charged particles and directs them into the transport line to the Debuncher. Particles not selected are passed to a beam dump.

6.2 The Debuncher

The Debuncher was designed to accept antiprotons fresh from the target and reduce their momentum spread though RF bunch rotation and adiabatic debunching and reduce the transverse profile of the beam prior to injection into the accumulator through betatron stochastic cooling. The Debuncher is larger than the Accumulator by about 6.6% though they both share the same tunnel; for 53 MHz RF, the Debuncher has 90 buckets as opposed to the 84 chosen for the Accumulator (for compatibility with the Booster). The Debuncher is roughly triangular in shape with three straight sections of low dispersion.

The beam coming from the target still has the RF bunch structure of the Main Ring. Debuncher RF system 1 (DRF1), phase locked to the Main Ring RF, accepts the longitudinally short bunches (*i.e.* short in time) and rotates them in phase space so that they become small in momentum spread with a large time spread. The beam is then adiabatically debunched by reducing the RF voltage over a period of milliseconds. The bunch rotation lowers the momentum spread of the pbars to 0.2% from 4%.

Since the Debuncher has 90 RF buckets and the antiprotons must be injected into the Accumulator with only 84 buckets, there is room in the orbit for a longitudinal gap. This gap is desirable in that it allows injection and extraction with minimal loss caused by the rise and fall time of the kicker magnets. (Loss minimization is clearly of the highest order since the antiprotons are so difficult to accumulate.) The gap is maintained by a second RF system, DRF2.

Since the pbar cycle is at least 2.4 sec, there are more than two seconds of free time available in the Debuncher after debunching and prior to preparing for the next batch of fresh antiprotons. The choice was made to devote two seconds of time to betatron stochastic cooling. Cooling reduces the phase space occupied by the beam and thus aids in fitting the beam into the smaller aperture of the Accumulator and reduces the amount of noise in the momentum cooling in the Accumulator by reducing the transverse oscillations of the beam.

In the regions of low dispersion (where transverse particle position is affected least by the particle's longitudinal momentum), beam pickups measure the transverse position of a particle. This is related to the betatron oscillations of the particle in question. The measurement results in a corrective signal being sent across the central section

of the ring to meet the particle whose position was just measured, and a corrective kick is made to reduce the amplitude of the betatron oscillations of the individual particle. The result of the corrective signal is small (~1 part in 10^6), however, this becomes significant when the beam makes ~10^6 turns per second.

This simple picture of stochastic cooling becomes complicated when more than one particle is involved, and several tricks are employed to maximize the cooling effect. The Schottky noise signals induced by other particles near the particle in question tend to make random adjustments to the given particle's orbit which will "heat" the particle instead of cooling it. The particle undergoes a random walk in phase space proportional to the square of the noise voltage and thus the square of the gain of the electronics; the effect of the particle on itself is linear with respect to amplifier gain. Thus, a small enough choice in signal gain allows the cooling signal to dominate over the noise. Clearly, if the bandwidth of the cooling system electronics (including the signal pickups) were sufficiently high, each particle could be resolved separately from all others. Thus maximizing the bandwidth of each cooling system is a priority. Within the accumulator, some cooling systems operate in range the of 4 - 8 GHz. Finally, the thermal noise within the cooling system electronics is also amplified and applied as corrections to the antiproton orbit. This effect is minimized by operating the systems at cryogenic temperatures.

A more intuitive picture of stochastic cooling can be achieved by considering that the cooling system responds only to the average behavior of a portion of the beam with a minimum size determined by the maximum available bandwidth of the cooling system. Particles closer than the maximum resolution of the system are unresolved, and thus it would seem that cooling could never be achieved. However, since all the particles are orbiting with slightly different frequencies, they can be resolved (statistically) after a finite number of turns. This randomization of particles due to mixing allows the cooling system to have a net cooling effect.

The magnitude of the betatron oscillations (and thus the transverse size) of the beam is lowered by a little more than a factor of two during stochastic cooling operations in the Debuncher.

The beam of antiprotons, now a fairly continuous ribbon (with a large gap) with a low momentum spread (about 0.2% or an energy spread of about 18 MeV), is finally injected into the Accumulator as the Debuncher prepares for its next batch.

6.3 The Accumulator

The Accumulator is roughly triangular in shape, like the Debuncher. The "vertices" of the triangle contain short straight sections instead of the smooth arcs in the Debuncher. Thus, there are six straight sections in the Accumulator yielding alternating high and low dispersion regions. Also like the Debuncher, the Accumulator operates above transition, such that the differences in particle momenta are seen primarily in their different path lengths. Higher momentum particles follow a larger radius orbit than the central orbit; lower momentum particles live in a smaller radius orbit. This difference in orbit radius is utilized in the cooling system in the Accumulator where the injected antiprotons are cooled over time and concurrently slowed to move into a smaller orbit within the machine.

The antiprotons are injected into the Accumulator onto a closed injection orbit which is about 80 mm to the outside of the central orbit. During the next 300 ms the injected beam is adiabatically captured by a 53 MHz RF system and decelerated by ≈60 MeV (0.7%) to the tail of the "stack" of previously injected antiprotons. The beam is then released and again debunched by adiabatically reducing the RF voltage. A profile of a typical antiproton stack is shown in Figure 10.

Once in the stack tail, momentum stochastic cooling decelerates the particles, pushing them into the stack core. The core is located about 63 mm inside the central orbit of the machine and is about 150 MeV lower in energy than that of the injection orbit. This process takes on the order of an hour to push the particles into the core. The pickup electrodes for this process are located in a region of high dispersion so that the beam is spatially separated due to the momentum differences of the individual particles.

Once in the core, three additional stochastic cooling systems act on the beam. The momentum cooling system controls the momentum spread of particles in the core. The betatron cooling systems act to control the vertical and horizontal distributions of the beam about the central core orbit. Once again, the momentum pickup electrodes are placed in a region of high dispersion while the betatron pickup units are positioned in a region of low dispersion. The increase in beam intensity within the stack core reflects the higher operating bandwidth of the cooling systems acting on the core as opposed to those operating on the stack tail.

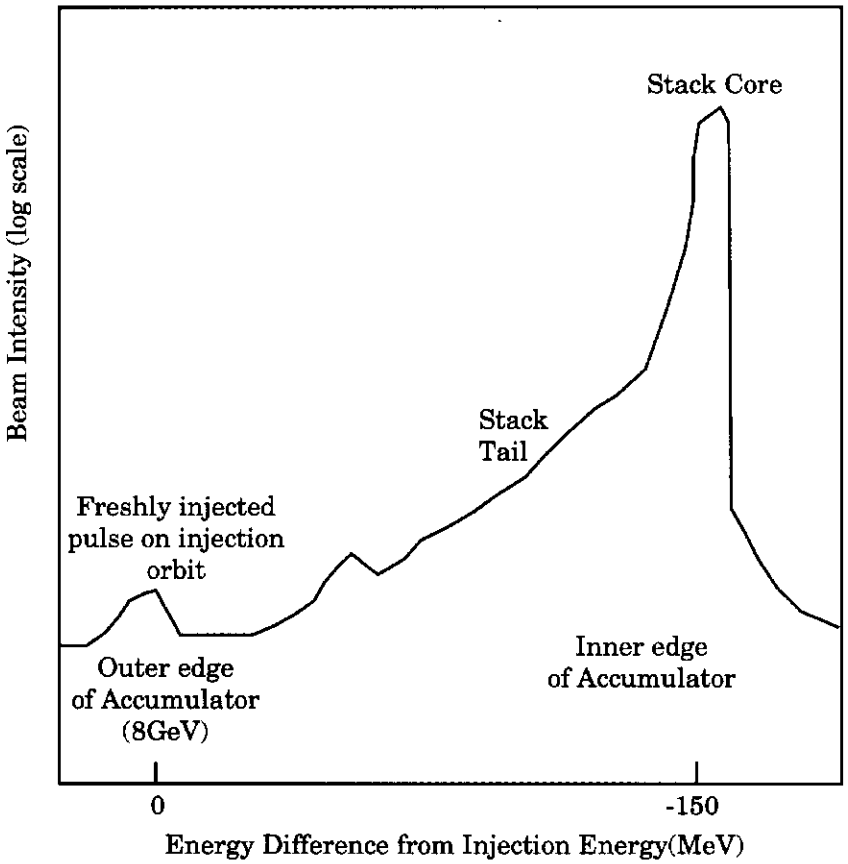

Figure 10 The profile of a typical antiproton stack in the Accumulator. The energy scale is relative to the energy of the injected antiprotons from the Debuncher.[18]

Once the Tevatron needs to be filled with antiprotons (assuming the number of antiprotons in the core is sufficient) a portion of the antiprotons in the stack core are moved to the extraction orbit (which is the same as the injection orbit). This is accomplished by an RF system with a harmonic of two (two RF buckets for the entire ring) but with one bucket suppressed. The system is powered on at a very low amplitude and at a frequency corresponding to the revolution frequency of the beam in the core. (The momentum spread ($\Delta p/p$) that can be captured by an RF system is related to the voltage applied to the RF cavities; thus, a very low power RF signal only captures a part of the core leaving the remaining pbars largely undisturbed.[21]) A portion of the core is captured and accelerated to place it in the extraction orbit where an additional two bucket RF system is energized to shrink the bucket longitudinally into the space occupied by eleven Main Ring buckets at injection. Finally, the Main Ring RF system is phase-locked to the 53 MHz accumulator RF system which is

energized to bunch the antiprotons into eleven RF buckets for synchronous transfer into the Main Ring.

7 The Tevatron

The Tevatron is a proton-antiproton colliding beam synchrotron accelerator delivering a center-of-mass energy of 1.8 TeV; it is currently the highest energy collider in existence.[2][22] It was commissioned as a proton synchrotron in 1983, breaking the world record for the highest energy man-made particle beam on July 3rd of that year with a 512 GeV beam. Because it was used to generate proton beams of 800 GeV for fixed target experiments, twice the 400 GeV energy previously delivered by the Main Ring, it is sometimes referred to as the Doubler. With the completion of the Antiproton Source, it became possible to operate the Tevatron as a colliding beam accelerator. First colliding beam tests were in October, 1985. The 1992-1993 run (Run IA) was the third operating run for the collider.

The Tevatron also happens to be the first large scale superconducting synchrotron to be constructed. All of the dipoles, quadrupoles, and correction magnets making up the basic lattice of the machine are superconducting and are cooled by liquid helium to a temperature of 4.6 K. Because of the electricity savings associated with using superconducting magnets, the Tevatron was originally dubbed the Energy Saver.

With the above exceptions, the Tevatron is actually quite similar to the Main Ring having 774 dipoles and 216 quadrupoles for the basic lattice of the machine. It has the same radius of 1000 m and is situated about 25.5 in below the Main Ring within the same tunnel enclosure. Its RF system operates at ~53 MHz yielding the same 1113 RF buckets as for the Main Ring. This results in a nearly 100% beam transfer efficiency between the two accelerators (as compared to an 85% - 90% transfer efficiency to the Main Ring from the Booster or pbar source).[15] It currently operates in a "six-on-six" mode where six bunches of protons and six bunches of antiprotons countercirculate in the ring with two luminous regions, B0 and D0. The peak luminosity for Run 1A was $\sim 1.0 \times 10^{31} / (\mathrm{sec}^2 \mathrm{cm})$.

At the beginning of each store, the six proton bunches ($\sim 150 \times 10^9$ protons each) are injected individually into the Tevatron followed by six antiproton bunches ($\sim 50 \times 10^9$ antiprotons each). Once injected, they are ramped together to the current operating

energy of 900 GeV per beam. Each bunch has an assigned location relative to the Tevatron Beam Sync marker. The bunches are not evenly spaced around the ring; even spacing is not possible because 1113 is not an integer multiple of six. Instead, the bunch spacing alternates between 186 RF buckets and 187. This results in a beam crossing every ~3.5 μsec; with each RF bucket corresponding to 18.8 nsec. The collider experiment clock systems are phase-locked to the Tevatron via the TVBS marker. In addition, Beam Position Monitors (BPMs) on either side of the experiments enable the clock systems to recheck themselves each beam crossing. (In the DØ control room, a clock system alarm is often the first indication of lost beam.)

Once at flattop, special superconducting quadrupoles (known as low-beta quadrupoles) located on either side of the two luminous regions squeeze the beams and reduce the local beta to ~0.25 m.[23] This dramatically decreases the beam spot size to $\sigma_{x,y} \approx 40\ \mu m$ which increases the luminosity; it is for this reason that B0 and D0 are referred to as luminous regions. During Run IA, the superconducting quads on either side of DØ were not of equal strength. This resulted in the unfortunate shifting of the center of the luminous region ~10 cm upstream from the center of the detector. (The center of the luminous region varied throughout the run as adjustments were made.) The actual longitudinal distribution of event vertices measured by the tracking chambers at DØ yielded $\sigma_z \approx 30\ cm$. The location of the nominal interaction point and the longitudinal distribution of the event vertices is actually a convolution of two distributions: one due to the uneven focussing of the beams discussed above, and the other due to the timing of the bunches. The center of the bunches do indeed pass through one another at the center of the detector. Corrections made to the low-beta quadrupoles during the period after the run have corrected the position of the nominal interaction point for future collider runs.

At flattop, the Tevatron continues to circulate the beams for several hours maintaining the beam energy at 900 GeV; this is known as a *store*. During a store, the luminosity decreases as various factors contribute to depleting the ranks within the bunches. This is not an exponential decay as one might expect; if treated as such, the instantaneous lifetime of the store increases with increasing time.[23] Ideally, the store is maintained until the run coordinator decides that a higher average luminosity can be obtained by stopping to begin a new store with two hours being the minimum downtime between stores. The length of a store is then somewhat coordinator dependent with 12 - 18 hours being normal. Occasionally a technical problem ends

the store abruptly prior to any decision to end it gracefully. The length of the average store in Run 1A was enhanced by the addition of electrostatic separators around the ring which separate the proton bunches from the antiprotons (transversely) except at the desired collision regions.

One final comment about the Tevatron involves the beam profile measurement known as flying wires. In this device, a thin carbon-fiber filament is flipped through the beam at a well-measured speed of ≈5 m/sec. This corresponds to ≈0.1 mm per revolution. Scintillator telescopes downstream of the flying wires then detect secondaries created in beam-wire collisions yielding information about the beam intensity profile. This measurement is important to the collider experiments because of the possibility of being sprayed with secondaries; this is sometimes the reason why the tracking chambers occasionally trip off during a store.

8 Acknowledgements

This note grew out of a description of the accelerator that I included in my dissertation[24] for completeness. In compiling the information, I found that there was no document accessible to the uninitiated which answered my many questions. I am grateful to the members of my defense committee who critiqued the original version of this text and who continue to inspire me as colleagues on the DØ experiment. (Michael Rijssenbeek and Guido Finocchiaro of the Stony Brook High Energy Group, and Marvin Johnson of the Fermilab Research Division.)

Many of the details presented here are not commonly known outside the small circle of dedicated professionals who designed and operate "the machine" and who tirelessly deliver the beam to the experimenters. Most notable contributions to this note were from Chuck Ankenbrandt (accelerator HQ), Dave McGinnis (booster), Jim Morgan (operations), Ralph Pasquinelli (pbar source), Stan Pruss (accelerator physics), and Chuck Schmidt (linac). Of course the inaccuracies contained herein are due to my misunderstanding, not theirs.

9 References

[1] F. T. Cole, M. R. Donaldson, D. A. Edwards, H. T. Edwards, and P. F. M. Koehler, "Design Report, Superconducting Accelerator," Fermi National Accelerator Lab internal note, (unpublished, 1979).

[2] "Design Report, Tevatron 1 Project," Fermi National Accelerator Lab internal note, (unpublished, 1984).

[3] D. Patterson, "The FNAL Linac," Fermi National Accelerator Lab internal note, (unpublished, 1986).

[4] C. W. Schmidt and C. D. Curtis, "A 50 mA Negative Hydrogen-Ion Source," *IEEE Transactions on Nuclear Science*, **NS-26**, 4120, (1979).

[5] C. W. Schmidt, "Review of Negative Hydrogen Ion Sources," *1990 Linear Accelerator Conference*, Albuquerque, NM, (Sep. 1990).

[6] C. W. Schmidt, FNAL, private communication.

[7] C. D. Curtis, *et al.*, "Linac H– Beam Operation and Uses at Fermilab," *IEEE Transactions on Nuclear Science*, **NS-26**, 3760, (1979).

[8] L. J. Allen, A. J. Lennox, and C. W. Schmidt, "Operational Experience with the Fermilab Linac," *16th International Linac Conference*, Ottowa, Canada (Aug. 1992).

[9] "Fermilab Linac Upgrade Conceptual Design Report Revision 4A," Fermin National Accelerator Lab internal note, (unpublished, 1989).

[10] E. J. N. Wilson, "Proton Synchrotron Accelerator Theory," CERN Publication 77-07, (Mar. 1977).

[11] E. L. Hubbard, *et al.*, "Booster Synchrotron," Fermi National Accelerator Lab internal note, TM-405, (Jan. 1973).

[12] J. Crawford, "Basic Booster for Beginners," Fermi National Accelerator Lab internal note, (unpublished, 1980).

[13] C. Hojvat, *et al.*, "The Multiturn Charge Exchange Injection System for the Fermilab Booster Accelerator," *IEEE Transactions on Nuclear Science*, **NS-26**, 3149, (June 1979).

[14] B. Webber, "The Debuncher and Its Tuning As Relates To Booster," Fermi National Accelerator Operations Bulletin No. 719, (Mar. 1979).

[15] J. Morgan, FNAL, private communication.

[16] A. Braun, T. Meyer, "The Main Ring Rookie Book," Fermi National Accelerator Lab internal note, (unpublished, 1991).

[17] D. A. Edwards, M. J. Syphers, *An Introduction to the Physics of High Energy Accelerators*, (John Wiley and Sons, NY, 1993).

[18] E. Harms, "The Antiproton Source Rookie Book version 0.2," Fermi National Accelerator Lab internal note, (unpublished, 1993).

[19] M. D. Church and J. P. Marriner, "The Antiproton Sources: Design and Operation," *Annu. Rev. Nucl. Part. Sci.*, **43**, 253, (1993).

[20] D. Möhl, G. Petrucci, L. Thorndahl, and S. van der Meer, *Physics Reports*, **C58**, 73-119, (1980).

[21] D. Pasquinelli, FNAL, private communication.

[22] P. Emma, "Tevatron Introduction" Fermi National Accelerator Lab internal note, (unpublished, 1984).

[23] J. Butler, FNAL, private communication.

[24] J. Thompson, Ph. D. Thesis, State University of New York at Stony Brook, *Search for the Top Quark in Muon + Jets Events at* DØ, (unpublished, 1994).